

## Supporting information

### **Cuprous thiocyanate as Inorganic Hole Transport Material for Carbon Based Flexible Perovskite Solar Cells.**

Samyuktha Noola<sup>1</sup>, Gyanendra Shankar<sup>2</sup>, Francesca De Rossi<sup>2\*</sup>, Emanuele Calabrò<sup>3</sup>, Matteo Bonomo<sup>1</sup>, Claudia Barolo<sup>1,4,5</sup>, Francesca Brunetti<sup>2</sup>

*1. Department of Chemistry, NIS Interdepartmental Centre and INSTM Reference Centre, Università Degli Studi di Torino, Via Pietro Giuria 7, 10125, Torino, Italy.*

*2. CHOSE, Department of Electronic Engineering, University of Rome Tor Vergata 00133, Italy.*

*3. Halocell Europe, Viale Castro Pretorio 122, Rome, 00185, Italy.*

*4. ICxT Interdepartmental Centre, Università degli Studi di Torino, Lungo Dora Siena 100, 10153 Torino, Italy.*

*5. Istituto di Scienza, Tecnologia e Sostenibilità per lo Sviluppo dei Materiali Ceramici (ISSMC-CNR), Via Granarolo 64, Faenza, RA 48018, Italy.*

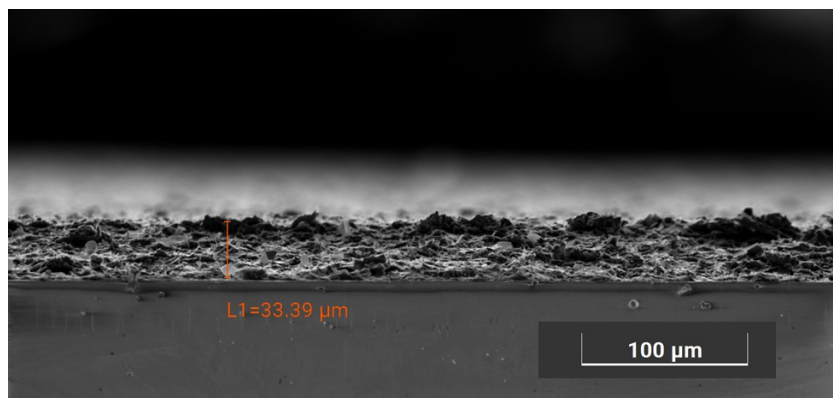


**Figure S1:** Cross-section SEM image showing the dry film thickness of the carbon top electrode.

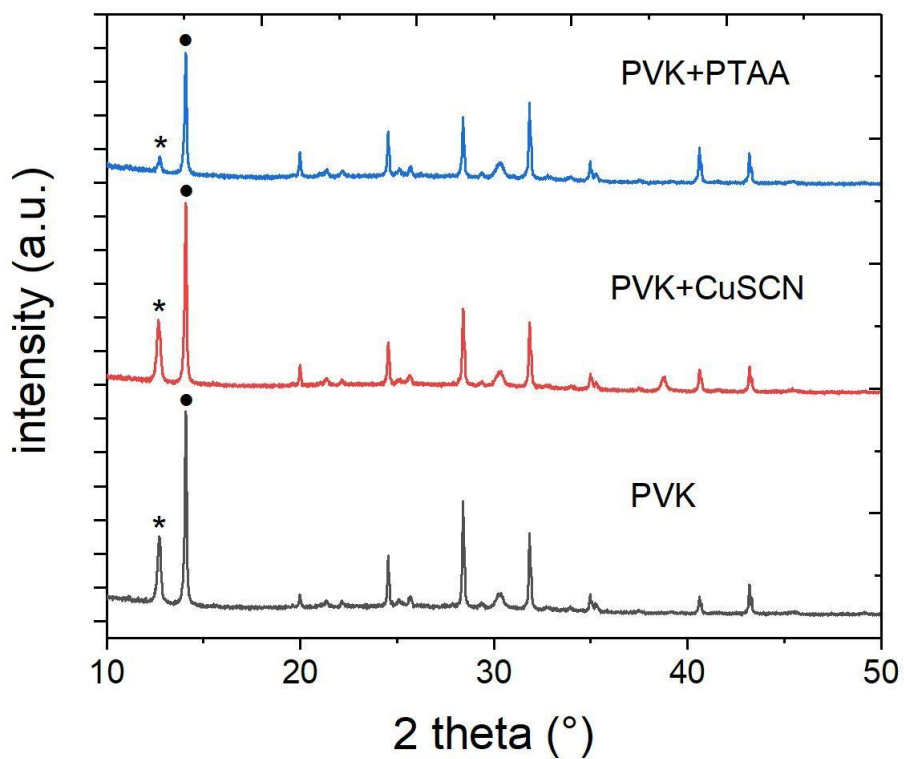


**Figure S2:** XRD diffraction patterns of the perovskite film (black), the perovskite film covered by the CuSCN layer (10 mg/ml, red), the perovskite film covered by the PTAA layer (12 mg/ml, blue), all deposited on glass/ ITO/ SnO<sub>2</sub>. Asterisks and solid dots indicate the 12.6° PbI<sub>2</sub> and 14.1° perovskite peaks.

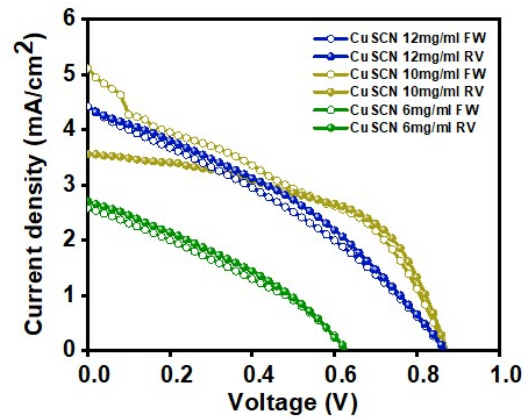


**Figure S3:** JV curves of F-PSCs with CuSCN at different concentrations using a gold top electrode.

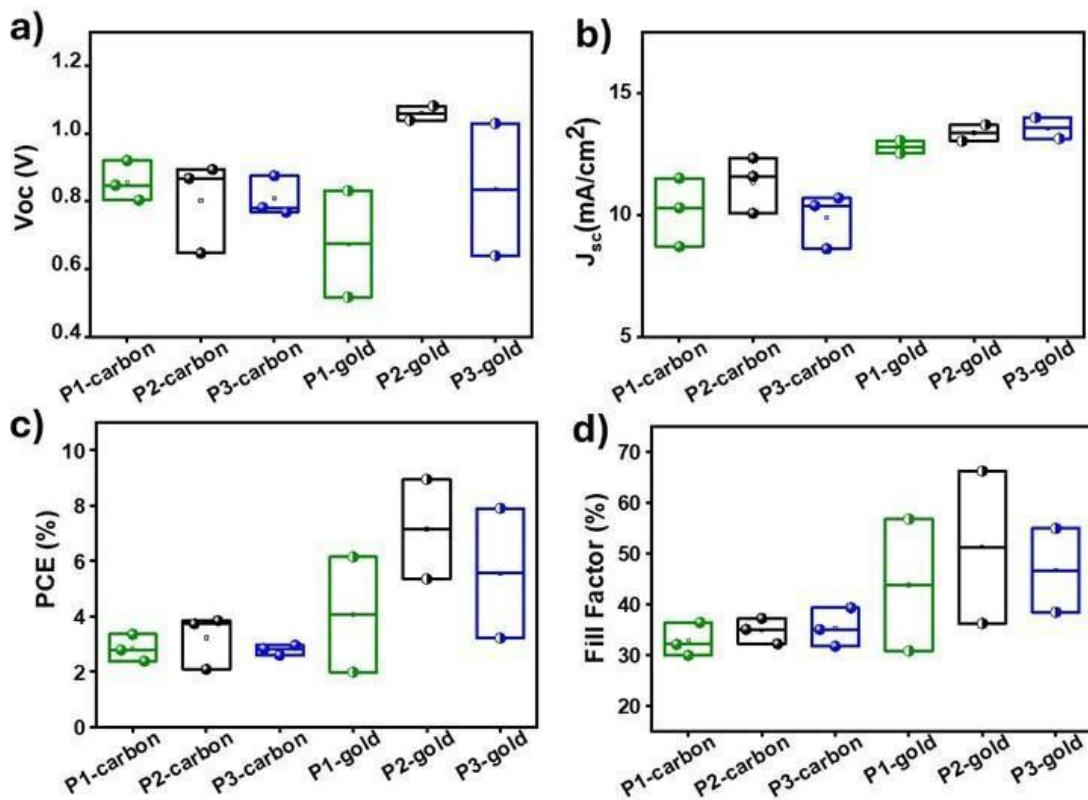


**Figure S4.** Photovoltaic parameters of flexible perovskite solar cells (PSCs) with an active area of  $1 \text{ cm}^2$  using different concentrations namely P1= 6 mg/ml, P2= 12 mg/ml, P3= 18 mg/ml of commercially available PTAA (MW= 105 kDa) with carbon and gold top electrode, measured under standard test conditions (STC, AM1.5G,  $1000 \text{ W/m}^2$ ,  $25 \text{ }^\circ\text{C}$ ).

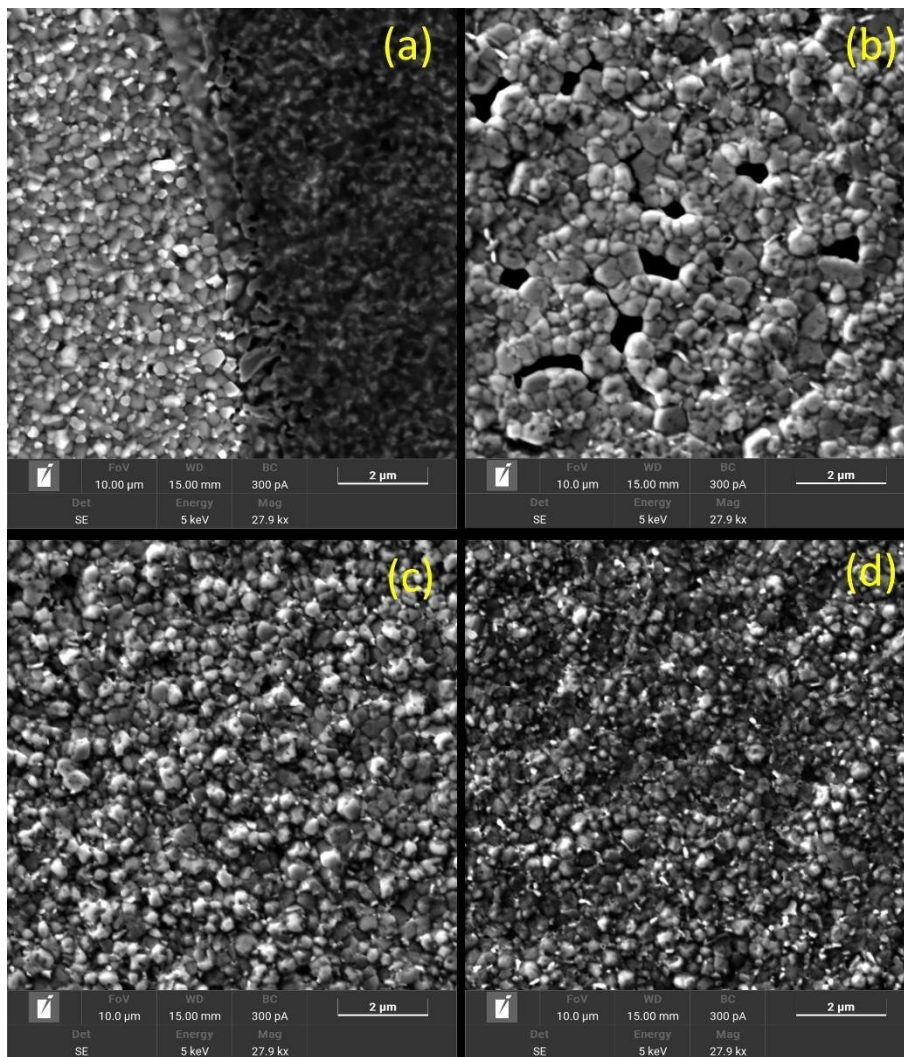


**Figure S5.** The top-view SEM images of: (a) the perovskite film partially covered by the PTAA layer, and the CuSCN layers at different concentrations: (b) 6 mg/ml, (c) 10 mg/ml, and (d) 12 mg/ml.

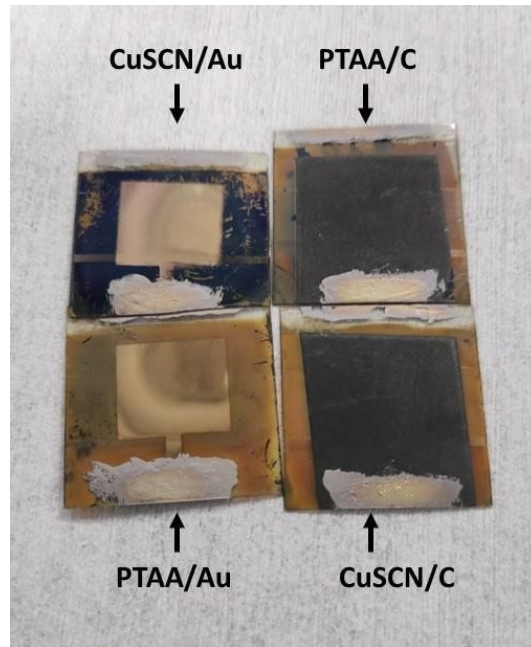


Figure S6: After one week of thermal stress ISOS T-1

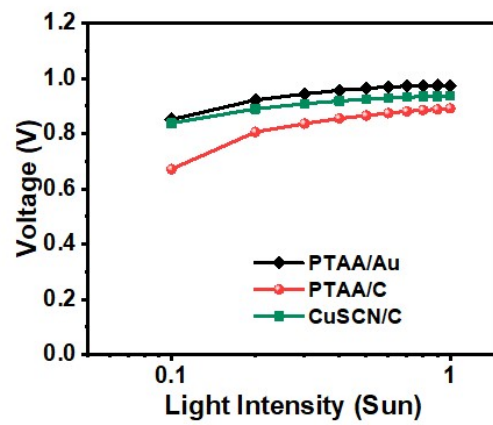


Figure S7:  $V_{oc}$  at different sun intensities.

**Table S1:** PV parameters of F-PSCs with CuSCN at different concentrations with gold top

concentration (mg/ml)	Scan	$V_{oc}(V)$	$J_{sc}(mA/cm^2)$	Fill factor (%)	PCE (%)
6	FW	$0.53\pm 0.06$	$12.1\pm 0.28$	$31.0\pm 2.80$	$2.01\pm 0.46$
	RV	$0.67\pm 0.22$	$12.7\pm 0.36$	$43.7\pm 18.3$	$4.06\pm 2.93$
12	FW	$1.05\pm 0.03$	$14.2\pm 1.51$	$48.0\pm 19.1$	$7.07\pm 1.88$
	RV	$1.05\pm 0.02$	$13.3\pm 0.46$	$51.0\pm 21.1$	$7.14\pm 2.54$
18	FW	$0.83\pm 0.27$	$13.1\pm 0.52$	$42.6\pm 12.1$	$4.95\pm 3.07$
	RV	$0.83\pm 0.27$	$13.5\pm 0.60$	$46.6\pm 11.6$	$5.56\pm 3.30$

electrode.

**Table S2:** Statistical data of Photovoltaic (PV) parameters of Gold F-PSCs employed with PTAA at three different concentrations.

Concentration CuSCN	Scan	$V_{oc}(V)$	$J_{sc}(mA/cm^2)$	Fill factor (%)	PCE (%)
6 mg/ml	FW	0.62	2.57	31.98	0.52
	RV	0.63	2.68	33.7	0.57
10 mg/ml	FW	0.86	5.10	35.85	1.58
	RV	0.87	3.54	52.8	1.63
12 mg/ml	FW	0.86	4.41	32.67	1.25
	RV	0.87	4.37	35.82	1.36

**Table S3:** Statistical data of Photovoltaic (PV) parameters of Carbon F-PSCs employed with PTAA at three different concentrations.

concentration (mg/ml)	Scan	$V_{oc}(V)$	$J_{sc}(mA/cm^2)$	Fill factor (%)	PCE (%)
6	FW	$0.86\pm 0.05$	$9.90\pm 1.38$	$32.2\pm 1.81$	$2.7\pm 0.34$
	RV	$0.85\pm 0.05$	$10.15\pm 1.40$	$32.7\pm 3.28$	$2.84\pm 0.48$
12	FW	$0.80\pm 0.13$	$11.31\pm 0.32$	$34.3\pm 4.58$	$3.19\pm 0.97$
	RV	$0.8\pm 0.13$	$11.31\pm 2.52$	$34.7\pm 2.52$	$3.22\pm 0.98$
18	FW	$0.80\pm 0.05$	$9.96\pm 1.05$	$35.9\pm 4.32$	$2.88\pm 0.43$
	RV	$0.80\pm 0.05$	$9.88\pm 1.12$	$35.2\pm 3.79$	$2.79\pm 0.18$

**Table S4:** Fitting parameters of EIS.

	PTAA/C	CuSCN/C
Chi-Sqr	0.009032	0.033705
Sum-Sqr	0.71354	2.7975
R1( $\Omega$ )	64.12	34.09

R1(Error)	1.6159	2.7722
R1(Error%)	2.5201	8.132
R2( $\Omega$ )	1253	1860
R2(Error)	75.747	83.729
R2(Error%)	6.0453	4.5016
CPE2-T(F.cm <sup>-2</sup> )	1.52E-07	2.77E-07
CPE2-T(Error)	2.03E-08	4.53E-08
CPE2-T(Error%)	13.338	16.346
CPE2-P	0.92906	0.82475
CPE2-P(Error)	0.014868	0.014524
CPE2-P(Error%)	1.6003	1.761
R3( $\Omega$ )	478.6	349.9
R3(Error)	105.55	149.22
R3(Error%)	22.054	42.646
CPE3-T(F.cm <sup>-2</sup> )	4.04E-05	5.79E-05
CPE3-T(Error)	2.19E-05	8.27E-05
CPE3-T(Error%)	54.21	142.86
CPE3-P	0.73677	0.88414
CPE3-P(Error)	0.15013	0.36845
CPE3-P(Error%)	20.377	41.673

#### References:

1. Dong, H., Ran, C., Gao, W. *et al.* Metal Halide Perovskite for next-generation optoelectronics: progresses and prospects. *eLight* **3**, 3 (2023).
2. Haeger, T., Heiderhoff, R. & Riedl, T. Thermal properties of metal-halide perovskites. *J. Mater. Chem. C* **8**, 14289–14311 (2020).